Neural signatures of declarative memory cueing using odors during sleep

Andrea Sánchez-Corzo[1,2,3,4]#, David M Baum[3,4]#, Martín Irani[3,5], Svenja Hinrichs[6], Renate Reisenegger[3,7,8], Grace A. Whitaker[3,9], Jan Born[6,10], Jens G Klinzing[6,10]*, Ranganatha Sitaram[2,3,4]*

# Equally contributing first authors
* Equally contributing senior authors

1. Centro Interdisciplinario de Neurociencias, Pontificia Universidad Católica de Chile, Santiago de Chile, Chile.
2. Multimodal Functional Brain Imaging and Neurorehabilitation Hub, Diagnostic Imaging department, St. Jude Children's Research Hospital, Memphis, TN, United States.
3. Laboratory for Brain-Machine Interfaces and Neuromodulation, School of Medicine, Pontificia Universidad Católica de Chile, Santiago, Chile.
4. Institute of Biological and Medical Engineering, Pontificia Universidad Católica de Chile, Vicuña Mackenna 4860, Macul 7820436, Santiago, Chile.
5. Department of psychology, University of Illinois Urbana-Champaign, IL, United States.
6. Institute of Medical Psychology and Behavioral Neurobiology, University of Tübingen, 72076 Tübingen, Germany.
7. Department of Neurophysics, Philipps-Universität Marburg, Marburg, Germany.
8. Centre for Mind, Brain and Behavior, Philipps-Universität Marburg and Justus-Liebig-Universität Giessen, Giessen, Germany.
9. Advanced Center for Electrical and Electronics Engineering, Federico Santa María Technical University, Valparaíso 1680, Chile.
10. Centre for Integrative Neuroscience, University of Tübingen, 72076 Tübingen, Germany.

Abstract

Long-term memories are formed by repeated reactivation of newly encoded information during sleep. This process can be enhanced by using memory-associated reminder cues like sounds and odors. While auditory cueing has been researched extensively, few electrophysiological studies have exploited the various benefits of olfactory cueing. We used high-density electroencephalography in an odor-cueing paradigm that was designed to isolate the neural responses specific to the cueing of declarative memories. We show widespread increases in the rate of sleep spindles, their duration, and their peak amplitude as an early response to odor cues. Spindle rates increased specifically around slow oscillation up states. We report further and partly surprising effects of cueing in lower frequency bands. Our results demonstrate the feasibility of studying memory-specific brain responses to olfactory cueing and identify sleep spindles as the prime candidate mechanism behind memory processing.

Introduction

Recently encoded information must undergo active consolidation during sleep to converted into long-term memories[1–3]. Reactivation results in a restructuring and strengthening of new

memories, a process called memory consolidation. One way to probe this process is a technique called cued memory reactivation, in which sensory reminder cues, like odors[4,5] or sounds[6–8] are presented during memory acquisition to associate them with the learned content. If the cues are presented again during subsequent sleep, this directs the process of consolidation towards the associated memories and improves their recall the next day[9]. Cueing with odors has a series of advantages over using sounds. By bypassing thalamic relays, olfactory inputs reach the neocortex and hippocampus more directly than other modalities[10] and tend not to disturb sleep[11]. Sounds in turn more easily allow for high numbers of different cues within a single experiment. They are independent of breathing, have clearly defined on- and offsets, and evoke stereotypical neuronal responses. Auditory cueing is therefore often considered more suitable for neuroscientific investigations, leading to a scarcity of electrophysiological studies using odor cueing[9].

The few existing electrophysiological studies on odor cueing showed that successful cueing is associated with changes in a series of neuronal activity patterns. This includes slow oscillations (SOs, ~1 Hz), slow waves (0.5-4Hz, including delta power), sleep spindles [12–16], and SO-spindle coupling strength[14]. These oscillations are known to be associated with cognitive functions, including the sleep-associated consolidation of memories[1]. Cueing effects on oscillatory patterns likely depend on the precise task to be memorized, cueing modality, and analysis technique. This is reflected in a spread of the demonstrated effects across various brain areas, frequency bands, and time delays relative to the cue, as well as some failed attempts to find robust associations between neural responses and memory improvements[9]. On the other hand, electrophysiological patterns in response to odor cueing have also been reported in studies where behavioral measurements show no significant benefit to memory[12,13].

In this study, we aimed at deepening the characterization of electrophysiological features associated with odor-cueing of declarative memories during sleep. For this purpose, we contrasted responses to two different odors. Before sleep, each odor was associated either with memories encoded during a declarative object-location memory task or with a procedural random finger-tapping task. The latter task did not contain any learnable sequences and was designed to at most induce sensory-motor learning. We conducted high-

density electroencephalographic (EEG) recordings during subsequent sleep, while in each of two nights, either one of the two odors was presented. We compared neuronal responses to the two odors with the goal to unravel neuronal activity specific to the cueing of declarative memories. Although memory performance was similar after both nights, independently of the odor presented during sleep, we demonstrate widespread increases in the rate of sleep spindles as an early response to declarative odor cueing. These increases were tightly coupled to SO up states. Moreover, the duration and peak amplitude of spindles increased over frontal areas. Unexpectedly, low-frequency power (< 8 Hz) increased at odor onset with this increase even slightly preceding odor onset. In summary, we demonstrate the feasibility of investigating declarative memory-specific neural responses to odor cues. Our results point towards an essential role of spindles not only in spontaneous but also externally induced memory reprocessing.

Methods

Participants

Twenty-three young adults between 19 and 25 years of age (12 females; 22 ± 2.0 years) participated in the study. Exclusion criteria were smoking, a diagnosed psychiatric disorder, ongoing medication, shift work, and a body-mass index (BMI) higher than 25. Participants were required to have a normal sleep-wake rhythm (i.e., going to bed between 10:00 p.m. and 1:00 a.m. and getting up between 6:00 a.m. and 9:00 a.m.). Participants were instructed to abstain from alcohol, naps, excessive exercise, extreme stress, as well as caffeine after 2 p.m. on the days of the experiment. Additional 29 participants were recruited but did not complete the study due to termination of the experiment for personal reasons or schedule incompatibility (n = 4), sleepless adaptation night (n = 3), illness (n = 3), insufficient learning performance (see below; n = 2), exceeding the maximum time to fall asleep (60 min; n = 1), insufficient deep sleep (< 20 min within 90 min of sleep; n = 14), or technical problems (n = 2). Participants received a compensation of 170 € for completing all experimental nights. The study was approved by the ethics committee of the medical faculty of the University Tübingen. All subjects gave their written informed consent.

Experimental Design

The study consisted of an adaptation night and two experimental nights. The adaptation night allowed familiarization with sleeping with the high-density EEG system and face masks. Participants did not perform any memory tasks and were not presented with odor during that night. The adaptation night was performed 1-14 days before the first experimental night, and the second experimental night 14-28 days after the first. **Figure 1** shows a scheme of the experimental design.

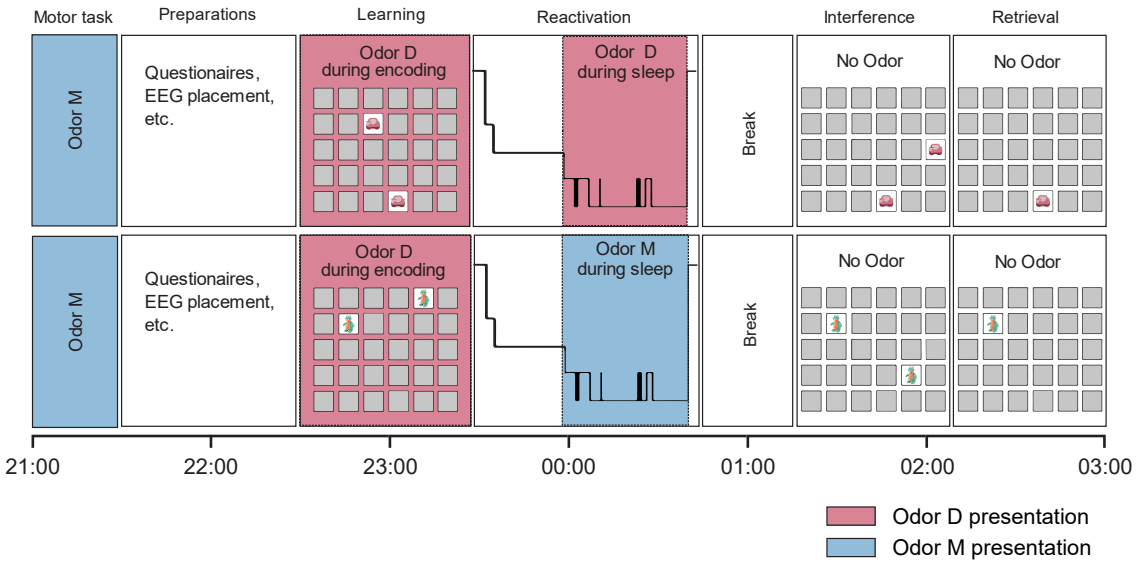

Figure 1: Experimental Paradigm. *Participants completed two experimental nights in which they first performed a procedural Random Reaction Time Task in the presence of Odor M. After a break, participants learned a declarative memory task while administered with a different Odor D. Subjects went to bed and slept while their brain activity was recorded using high-density EEG. Once participants reached deep sleep, they received odor stimulation, either with Odor D or Odor M, depending on the condition (the order of which was counterbalanced across participants). Subjects were woken up and performed an interference task, after which retrieval performance on the original task was tested.*

During experimental nights, participants first (at around 7:30 p.m.) performed a finger-tapping task with no learnable sequences (Random Reaction Time Task, RRTT). During this task, they were stimulated via a face mask with an odor defined as the "Motor task-associated odor" ("Odor M"). Two hours after the RRTT, participants learned a declarative memory task while being stimulated with an odor defined as the "Declarative task-associated odor" ("Odor D"). During the learning period and after all images had been presented twice, subjects completed the encoding of the image locations by performing an immediate recall test. The

test was repeated up to 5 times until the participants answered more than 60 % of the cards correctly. The percentage of correct responses in the last run represents the accuracy of learned paired locations before going to sleep. If participants did not reach 60 % performance after the last run, the experiment was ended and their data discarded (see 'Participants' section).

Upon reaching slow-wave sleep (SWS), either Odor D (in Night D) or Odor M (in Night M; balanced crossover design) was presented for windows of 15 s. Odor presentation was alternated with an odorless vehicle with 15-s breaks in between (resulting in a sequence of 15 s odor, 15 s break, 15 s vehicle, 15 s break, and so on). Stimulation was stopped when participants shifted from SWS to another sleep stage or woke up. Once participants had slept for a maximum of 90 minutes and received between 40 and 80 stimulations (either odor or vehicle), subjects were woken up and were shown a movie for 30 min to allow shaking off sleep inertia. Subsequently, they learned an interference task (see below) without any odor presentation. This was followed by another 45-min movie break before testing the participant's performance on the pre-sleep declarative memory task. Participants were tested for a single run. The experiment ended between 2:00 and 4:00 a.m. The subjects slept until the morning without EEG monitoring or further experimental procedures.

For analyses not reported here, participants also underwent an anatomical magnetic resonance imaging scan before the experiment and three 10-min resting-state recordings throughout each experimental night. Citral and Isobutyraldehyde (Merck Sigma Aldrich) were used for Odors D and M in a counterbalanced fashion.

Random Reaction Time Task (RRTT)

Participants performed a motor task with visual cues (four different displayed keys) as instructions for pressing corresponding keys on a keyboard with predefined fingers (excluding the thumb). The task was similar to the classic "Serial Reaction Time Task" but without any predefined repeating patterns. This made it impossible to improve performance by learning any sequences of keys, which was meant to minimize the encoding of new memories other than sensory-motor learning. Incorrect keystrokes were signaled to the participant. The test was performed in two blocks of five minutes each with a short break in

between. Throughout the task, the motor task-associated odor (Odor M) was presented to the participant in an intermittent fashion (15 s on, 15 s off). One goal of the RRTT was to expose the participants to Odor M during an engaging task and thereby make it comparable to Odor D in terms of pre-sleep familiarity. Task length and odor stimulation were chosen to structurally mimic the declarative memory task.

Declarative memory task

Participants also performed a two-dimensional object-location memory task used in previous studies[4,5]. This task is an adaptation of the social game "Concentration" or "Memory". A board with 30 gray squares in a 5 x 6 matrix represented 15 face-down pairs of cards. Cards showed everyday objects and animals in color. For the two nights, two different sets of cards and card locations were used. During *Learning*, card pairs were revealed one by one, such that the first card was shown for 1 s after which also the second card was revealed for another 3 s. Next, both cards were turned face down and the next card pair was revealed. This continued until all card pairs were presented twice. For a subsequent *immediate recall test*, subjects were presented with the first card of a pair and were asked to indicate the location of the second card using the mouse pointer. Correct responses triggered a green tick mark, which appeared for 1 s at the location of the selected card. Incorrect responses triggered a red cross and the correct card location was revealed for 3 s. Immediate recall was repeated until the participants showed a performance of at least 60 % correct responses (learning criterion) but not more often than 5 times. In a later *interference* version of the task, participants repeated the learning procedure using cards with the same images but the second card of each pair was placed at a different location[17,18]. This AB-AC learning scheme (A, B, and C correspond to different localizations) was used to test the stability of the original memory against partly overlapping and thereby interfering information. During the interference task, the subjects wore the odor mask but no odor was applied. Finally, participants performed another single run of the recall test using the card locations of the original task version. No direct feedback was given during the final recall. Only at the very end, the overall performance was shown. Task performance was measured by the percentage of the number of correctly recalled card pair locations after sleep (recall test) relative to the number of correctly recalled pair locations before going to sleep (learn lest) as a percentage: Recall Test / Learn Test * 100. Performance

was measured by the percentage of the number of correctly recalled card pair locations after sleep (recall test) relative to the number of correctly recalled pair locations before going to sleep (learn lest) as a percentage: Recall Test / Learn Test * 100.

Data acquisition

EEG data were acquired using a 129-electrode high-density EEG system (Electrical Geodesics Inc., Eugene, United States) with electrodes placed according to an adapted 10-10 system (HydroCel Geodesic Sensor Net). Data were recorded at a sampling rate of 1000 Hz and online-referenced to the vertex electrode. The location of each electrode in relation to the head was registered using optical tracking (Localite TMS Navigator, Localite GmbH, Bonn, Germany). For this purpose, structural T1-weighted magnetic resonance (MR) images were acquired, which allowed reconstructing each participant's individual head shape (1 mm^3 voxel size; MAGNETOM Prisma^{fit} scanner, Siemens Healthcare GmbH, Erlangen, Germany). In the beginning of the first experimental night, three optical references (small reflective tracking balls with defined relative positions, provided by the manufacturer) were attached to the participant's head. This was done by fixing them to an individually molded martial arts mouth guard, which allowed a precisely reproducible connection to the head. The reference balls, as well as a large number of points on the scalp were localized in space using an optically trackable pointing device. Reference balls and scalp locations were then coregistered with the surface of the reconstructed head model. Subsequently, the positions of all EEG electrodes were registered and added to the resulting common coordinate system. In the beginning of the second experimental night, mouth guard and attached tracking balls were placed again, correspondence with the participant's head surface was validated, and all EEG electrodes were placed at their respective location in the first experimental night. This procedure ensured that each electrode was placed over the same brain area in both sessions.

Sleep scoring and sleep architecture

Data were scored according to the Rechtschaffen & Kales (1968)[19] scoring criteria based on channels equivalent to C3/C4, referenced to the averaged mastoid channels, as well as bipolar EOG and EMG. To aid sleep scoring, data were bandpass-filtered between 0.3-35 Hz and

downsampled to 200 Hz. Each 30-s epoch was then labeled as Awake (W), Stage 1-4 (S1-S4), Rapid Eye Movement sleep (REM, R), or Movement Time (MT).

In order to evaluate the impact of cueing on sleep architecture, we compared the time spent in each sleep stage as well as sleep onset latency, time awake after sleep onset, number of arousals and sleep efficiency defined as the percentage of sleep after lights out.

Pre-processing of EEG recordings

EEG data were preprocessed using the FieldTrip toolbox[20]. Datasets were first segmented into epochs of -5 to 15 s around stimulus onset. Epochs with a stimulation duration of less than 15 s were discarded (2.46 ± 2.54 %, mean ± SD). Subsequently, data were low-pass filtered at 30 Hz using a finite impulse response (FIR) filter. An additional median filter was applied with an order of 30 to suppress occasional non-sinusoidal technical artifacts. Electrodes located on the face or neck were discarded from further processing. Noisy EEG channels were visually identified and interpolated using a distance-based weighted average of the neighboring channels (proportion of interpolated channels: 1.14 ± 2.72 %, mean ± SD). All data were visually inspected for artifacts. Identified artifacts led to rejection of the entire trial in case several channels were affected (1.67 ± 5.32 %, mean ± SD), while in the case of short, channel-specific artifacts, trial-specific channel interpolation was performed (3.28 ± 7.52 %, mean ± SD). For all subsequent analyses, data were re-referenced to the averaged signal from both mastoid electrodes. In datasets where mastoid channels were identified as noisy, the channel closest to the affected one was used as a replacement. Finally, data were downsampled to 250 Hz.

Event detection

Peak sleep spindle frequencies differ substantially from person to person. The peak frequency of spindles for each participant was identified individually using data from the central electrodes, where fast spindles are usually most pronounced (**Supplementary Figure 2A**). Irregular Resampling Auto-Spectral Analysis (IRASA)[21] was performed to separate the fractal from the oscillatory component for all data recorded during NREM sleep. For each participant and recording night, the maximum power of the oscillatory component in the frequency band between 12 and 16 Hz was used as the spindle peak frequency. This procedure reliably

resulted in fast spindle peaks (13.79 ± 0.38 Hz mean ± SD). Secondary slow spindle peaks were visible for some participants, but were too unreliable across the entire sample to be used for further analysis.

Discrete sleep spindles were detected separately for each channel using a MATLAB custom script based on published methods[18]. The EEG signal was bandpass-filtered around the detected individual spindle peak frequency (± 1.5 Hz). The signal's root-mean-square (RMS) was calculated using a sliding window of 0.2 s with a step size of one sample. Additional smoothing was performed with a sliding-window average of the same size. Time frames were considered spindle candidates if a) the RMS signal exceeded the value of the mean + 1.5 standard deviations (SDs) of the RMS signal of all combined stimulation epochs for a period between 0.5 and 3 s and b) the RMS signal inside this period crossed a second amplitude threshold placed at mean + 2 SDs for at least one sample.

Individual slow oscillations (SOs) were detected automatically using a custom script based on spectral content and duration. The detection procedure was largely based on prior literature[18]. In detail, the EEG signal was bandpass-filtered to the slow-wave (SW) frequency range (0.5 - 4 Hz) using a zero-phase two-pass Butterworth filter with an order of 3. Candidates for SOs were identified by the presence of two consecutive negative-to-positive zero crossings, framing a negative and a positive half-wave, separated by the positive-to-negative zero-crossing inside this time window (**Supplementary Figure 3**). These candidates were further validated using three required characteristics: I) Negative half-waves needed to cross a threshold trough amplitude of 1.1 standard deviations from the average of the entire signal inside of analyzed trials; II) peak-to-peak amplitudes of candidates needed to cross a threshold of 1.1 SDs from the average peak-to-peak amplitudes of the entire signal inside of analyzed trials; III) consecutive positive-to-negative zero-crossings needed to be separated by 0.8 to 2 seconds. From the resulting set of detected SOs, outliers with trough amplitudes beyond the median ± 3 SDs across all detected slow oscillations were discarded. The SO slope, as an established metric, was defined as average of slopes over samples between the negative peak and positive peak of the SO.

Validation of detected events

The spindle and slow oscillation detection procedures were evaluated based on: I) The topographic distribution of the detection rate of events across the scalp (**Figure 2A** and **3A**); II) the average waveform and spectral composition of the raw signal (**Figure 2B** and **3B**) incl. where spindles reached their peak amplitude (**Figure 2C**); III) the occurrence rates of events across sleep stages (**Figure 2D** and **3C**); IV) the occurrence of detected spindles along detected slow oscillations (i.e., proportion of SOs having a nested spindle (**Figure 4B**) and phase-amplitude coupling (**Figure 4C**); spindle time points were based on the event's midpoint, half way between its on- and onset). Evaluations were done for all events during S2-S4.

Event-coupling: spindles and SO

Slow oscillations tend to couple sleep spindles to their up phase. To analyze changes in this coupling, the signal was bandpass-filtered between 0.5 and 2 Hz and Hilbert transformed. Based on the resulting analytic representation of the signal, the phase was extracted at the midpoint of each detected sleep spindle (half way between its on- and onset). Spindles were considered to occur along an SO when their midpoint was located between the SO onset and offset (positive-to-negative zero crossings).

Time-frequency analysis

Time-frequency transformation was performed between -5 and 15 s (steps of 100 ms) around stimulation onset and between 0.7 and 20 Hz (steps of 0.1 Hz). Morlet wavelet were used in steps of 100 ms and with a frequency-dependent width between 5 s for the lowest frequency and 0.5 s for the highest frequency. Time-frequency data were Z-scored using mean and SD across all concatenated vehicle trials of the same night [22]. Power values were then averaged for each time point in the slow wave (0.7 - 4 Hz), theta (4 - 8 Hz) and spindle (10 - 15 Hz) band. Then, the power over channels was averaged in an anatomically-defined central cluster and thereby obtained a single time series for each frequency band of interest.

For analyzing spindle power around SOs, a similar analysis was performed. For this, Morlet wavelets with a width of 12 cycles were used with temporal steps of 50 ms on 6-s time windows centered around detected SO down states. Power was estimated in steps of 0.05

Hz, centered around the average of individual spindle peak frequency (13.80 ± 0.38 across subjects, mean ± SD). The first and last seconds of the time window served as padding and were removed to avoid edge artifacts. Power estimates obtained during each SO event belonging to odor stimulation periods were normalized similarly to the analysis above where SO events belonging to vehicle periods served as vehicle trials.

Statistical analysis

If not otherwise noted, all statistics were performed using two-tailed tests and reported p values were corrected for multiple comparisons.

Event detection and features. Occurrences of spindles and SOs across sleep stages were analyzed by averaging their rates over channels within anatomically-defined clusters and comparing them between sleep stages using the Kruskal-Wallis test. For analyzing differences in event characteristics between conditions, metrics obtained during odor stimulation were Z-scored using the mean and SD obtained across all vehicle trials of the same night. As a result, each odor trial was normalized by a common vehicle baseline. The two odor conditions were then compared using either a whole brain analysis or a confined subset of electrodes. The latter was done in cases a) where there was a clear hypothesis about the anatomical distribution of a potential effect (anatomically defined cluster) or b) where a post-hoc analysis of an effect found in the whole-brain analysis was performed. For whole-brain analyses, channels with significant differences between conditions (two-tailed paired-samples t-tests; sample-level alpha 0.05) were grouped into connected clusters and cluster-level statistics were calculated by summing up the t-values within each cluster. Subsequently, the found clusters were subjected to multiple comparison correction by comparing them to a reference distribution obtained using a Monte Carlo permutation approach (cluster-based permutation analysis as implemented in Fieldtrip; maxsum method; cluster-level alpha 0.05; 100,000 permutations)[23]. For analyzing channel subsets, Wilcoxon's rank sum tests were performed on the average across all channels in that cluster.

Event coupling. Differences in the coupling of spindles to slow oscillations were analyzed by comparing I) the number of coupled spindles, II) the phase consistency of this coupling, as well as III) shifts in the coupling phase. For all types of analysis, samples were normalized

subject-wise by subtracting the average of all vehicle trials from the average of all odor trials of the same night. For coupling consistency analysis specifically, differences in the numbers of detected events and therefore phase estimates (potentially leading to systematic biases[24]) were controlled for by running the analysis on 10,000 randomly selected subsets of equal size and averaging the results. Samples were compared using channel cluster-based analysis as described in the previous section. Angular data obtained from the phase-coupling analysis were processed using the circ_stat toolbox[25] and analyzed with the Watson-Williams multi-sample test implemented in Fieldtrip's cluster-based permutation pipeline.

Time-frequency analysis. Band-limited power time-series were statistically compared between conditions using two-tailed paired-samples t-tests (sample-level alpha 0.05), followed by multiple comparison correction following a non-parametric cluster-permutation approach (analogous to the event analysis described above; 10,000 randomizations; cluster-level alpha 0.05).

Behavioral performance. Differences in memory task performances between odor conditions were evaluated using the non-parametric paired Wilcoxon rank sum test.

Samples. Data were considered outliers if their normalized values were more than 3 SDs above or below the median difference between all normalized Odor D and Odor M values. Such data points were removed before statistical analysis, together with their sample-specific counterpart of the contrasted condition. Outlier rejection was not performed for the analysis of coupled events due to the low number of trials.

Results

Odor cueing of declarative memories enhanced spindle activity

We analyzed the effects of odor cueing of declarative memories on the detection rate, duration, and amplitude of sleep spindles detected during NREM sleep. We found that, in the first half (0 - 7.5 s) of the stimulation period, declarative memory cueing increased the rate of sleep spindles over centro-parietal brain areas (Odor D vs Odor M, cluster-level p = 0.007, **Figure 2E**), their duration over frontal areas (p = 0.028, **Figure 2F**), as well as a trend for increased peak amplitude over frontal areas (p = 0.090, **Figure 2G**). These effects were weaker or undetectable when considering the whole stimulation period (0 - 15 s, lowest cluster-level p = 0.089 for spindle rate, **Figure 2E**). To further illustrate these changes and estimate their effect size, we conducted a follow-up analysis on averages across electrodes within found clusters (Odor D vs Odor M, spindle rates: 0.15 ± 0.06 vs -0.08 ± 0.03, average ± SEM, p = 0.007, Wilcoxon's z = 2.702, **Figure 2E**; duration: 0.27 ± 0.07 vs -0.07 ± 0.0.07, p = 0.002, z = 3.098, **Figure 2F**; peak amplitudes: 0.20 ± 0.06 vs -0.04 ± 0.09, p = 0.027, z = 2.219, **Figure 2G**).

The process of detecting sleep spindles was assessed in a post-detection validation process illustrated in **Figure 2A-D** and the **Supplementary Figure 2**. As expected, I) detection rate of spindles was highest in centro-parietal electrodes (**Figure 3A**), II) the averaged signal showed a fusiform oscillatory activity in the sigma frequency band **(Figure 3B**), III) the maxima of the RMS signal preferably located around the event's midpoint (**Figure 3C**) and IV) detection rates were highest in S2 and decreasing towards S4 (**Figure 3D**).

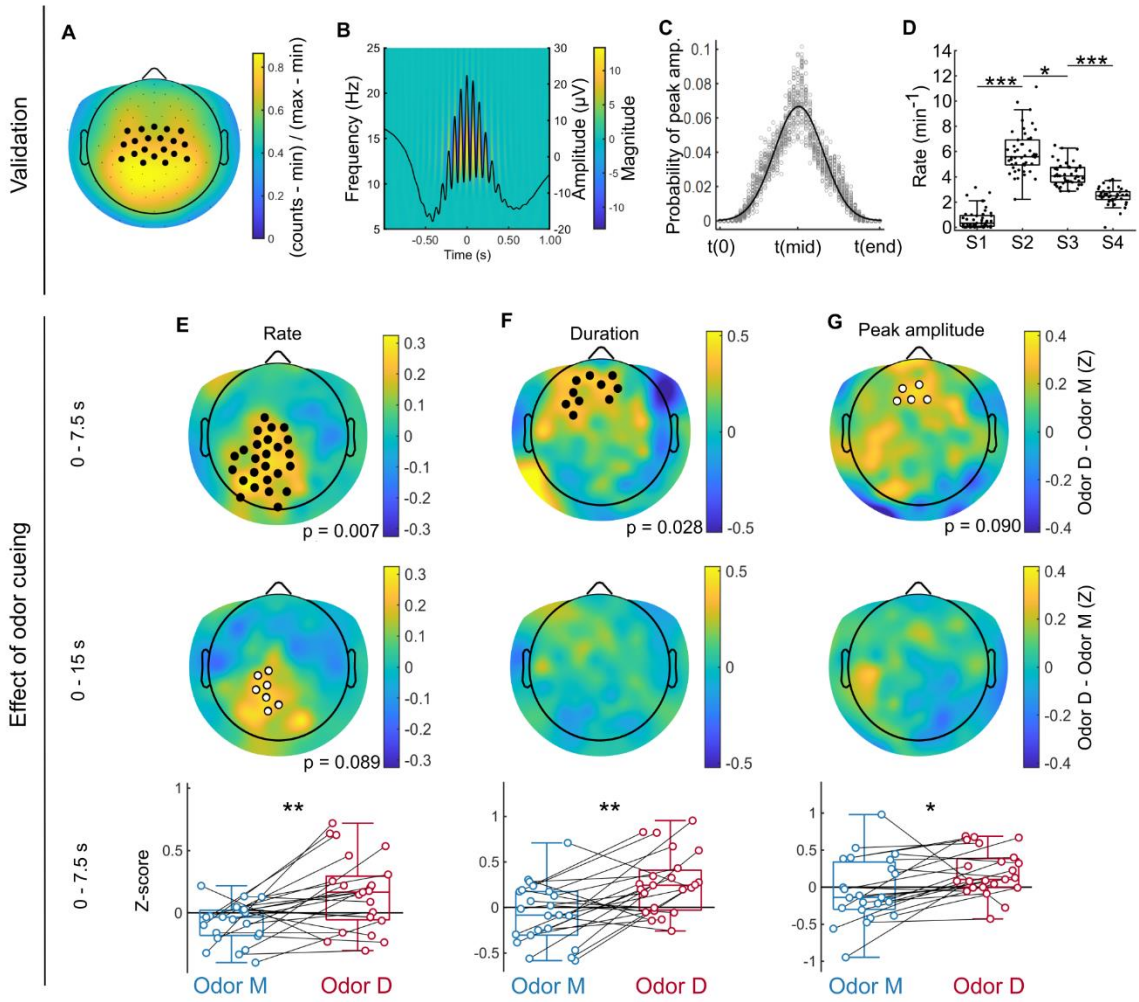

Figure 2: Odor cueing enhances several characteristics of fast sleep spindle activity. *Detected sleep spindle events were validated based on established characteristics such as distribution of detection rate across scalp electrodes (**A**), average waveforms and time-frequency composition (**B**), location of spindle signal peaks (**C**; t(0), t(mid) and t(end) refer to onset, midpoint and offset times), as well as their detection rates across different sleep stages (**D,** S1: 0.65 ± 0.12, S2: 5.93 ± 0.25, S3: 4.22 ± 0.13, S4: 2.47 ± 0.11, average ± SEM respectively). Black circles in A represent electrodes belonging to the anatomically-defined central cluster used for validation steps in **B**-**D**. Cueing with Odor D (red) compared to Odor M (blue) was associated with significant increases in spindle rate (**E**) and duration (**F**), as well as a trend for their maximum amplitude (**G**). These effects were present specifically in the first half (0 - 7.5 s) of stimulation (0 – 7.5 s; **E**-**G** top panels) but were not detectable when analyzing the entire stimulation window (0 - 15 s; **E**-**G** middle panels). Boxplots (**E**-**G** bottom panels) display changes between Odor D and M in 0 - 7.5 s averaged over the clusters shown in the top panels. ***, p < 0.001; **, p = 0.007 and 0.002 for **E** and **F**; *, p = 0.017 and 0.027 for **D** and **G**, respectively. Lines connect subjects across the conditions.*

Declarative memory cueing enhances the amplitude of slow oscillations

After demonstrating that declarative memory odor cueing affected several characteristics of sleep spindles, we asked whether similar effects were apparent for slow oscillations. Indeed, declarative memory odor cueing resulted in a trend for more negative SO troughs (more negative peak amplitude of negative half wave) of centro-parietal SOs during the first half (0 - 7.5 s) of the stimulation period (Odor D vs Odor M: cluster-level p = 0.055, **Figure 3F**). Similar to the spindle analysis, this effect was weaker and not statistically significant when comparing the entire stimulation period (0 - 15 s). No changes were found for other SO event metrics such as rate and slope (**Figure 3D** and **3E**, respectively). A follow-up comparison of the average across all electrodes in the found cluster shows the size of this effect (Odor D vs Odor M: -0.19 ± 0.05 vs -0.01 ± 0.04, average ± SEM (non-inverted z scores), p = 0.015, Wilcoxon's z = 2.439, **Figure 3G**). The detection of SOs was evaluated similarly to detected spindles in a post-detection validation (**Figure 3A-3C**, **Supplementary Figure 3**).

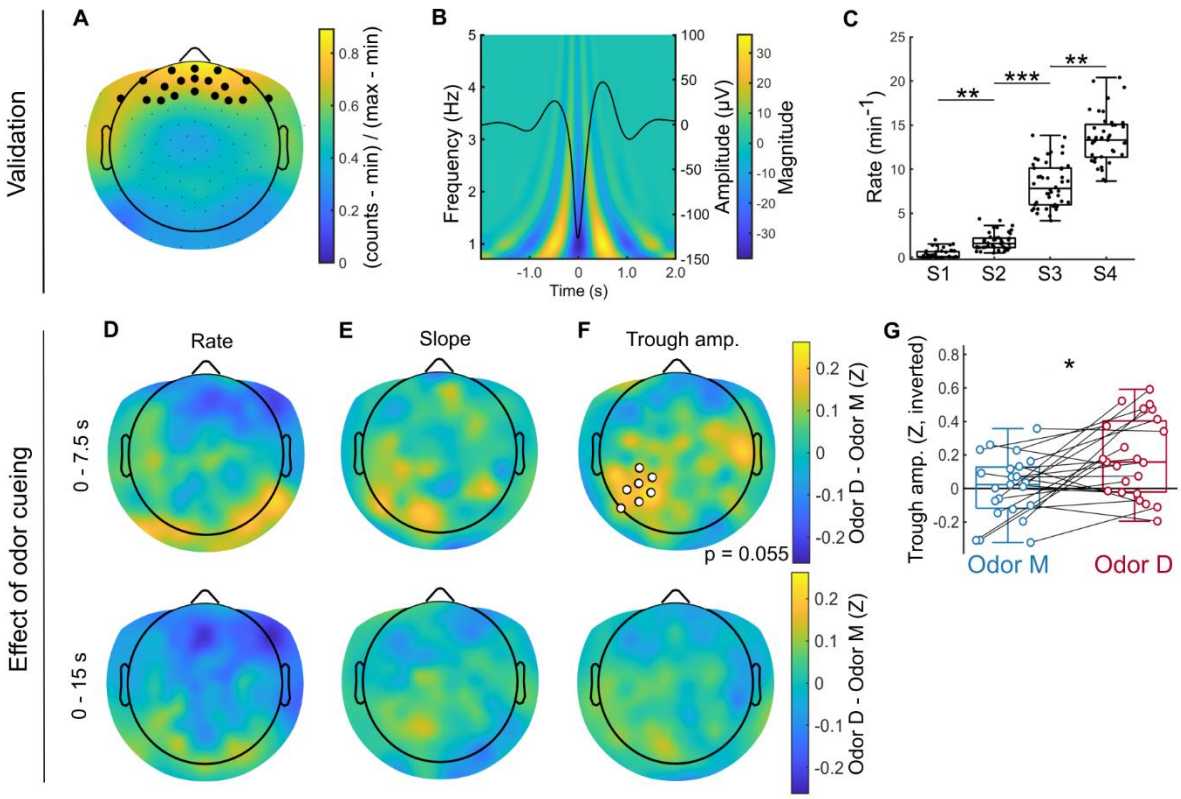

Figure 3: Declarative memory odor cueing increased the trough amplitude of posterior slow oscillations. *Detected slow oscillatory events were validated based on their canonical*

*characteristics using their distribution across the scalp (**A**), their averaged waveforms and time-frequency composition (**B**), as well as detection rates across different sleep stages (**C**, S1: 0.36 ± 0.08, S2: 1.78 ± 0.14, S3: 8.23 ± 0.38, S4: 13.54 ± 0.44, average ± SEM respectively). Black circles in **A** represent electrodes belonging to the anatomically-defined frontal cluster used for validation steps in **B** and **C**. Presenting Odor D did not evoke changes in event detection rate (**D**) or slope (**E**) when compared to Odor M, but resulted in more negative SO trough amplitudes (**F**, Z-scores are inverted for visual clarity) specifically in the first half (0 - 7.5 s, top panel) of the stimulation window (but not in the whole window, 0 - 15 s, bottom panel). This effect is further illustrated by comparing averages across all electrodes inside the found cluster (**G**, data shown for 0 - 7.5 s, lines connect data from the same participant). *, p = 0.015; **, p = 0.002 (S1 vs S2) and 0.006 (S3 vs S4); ***, p < 0.001.*

Declarative memory cueing increases the number of spindles co-occurring with an SO

Slow oscillations and sleep spindles show a temporal synchronization, such that SOs tend to nest sleep spindles to their depolarized up state (**Figure 4A**). Considering the spindle and SO changes induced by declarative memory odor cueing above, we now asked whether cueing further affected the synchronization of these events. Since cueing effects were most detectable during the first half of the stimulation period, we focused these analyses on this time window (analyses of the whole stimulation window are reported in **Supplementary Figure 4**). Since coupled events mainly occurred in and around central electrodes, we performed all analyses described below on averages across electrodes inside an anatomically defined central cluster (**Figure 4B**). Of all SOs detected in central electrodes, 8.8 ± 0.5 % (average ± SEM across subjects) had spindles that matched our criteria (**Figure 4C**). As expected, most SO-coupled spindles occurred around the SO up state. When dividing the SO cycle into seven bins of 51.4°, 83.7 ± 1.7 % of those spindles had their midpoint during SO up states (phase angles between 12.9° and 167.1°; see light green-shaded area in **Figure 4C**). This was the case in both odor conditions (see **Figure 4D** for the average preferred coupling angle for each participant, separated by Odor D and M). Interestingly, declarative memory odor cueing increased the number of spindles specifically around SO up states (between 12.9° and 167.1°, Odor D vs Odor M: 0.032 ± 0.011 vs 0.003 ± 0.008, average ± SEM, p = 0.022, z = 2.289, **Figure 4E**), while for other phase bins, spindle counts did not change significantly (-0.003 ± 0.008 vs -0.010 ± 0.004, p = 0.865, z = 0.170). The same effect was observed when analyzing coupled events across the whole odor stimulation period (**Supplementary Figure 4**).

We then investigated how the stronger accumulation of spindles around SO up states translates into phase coupling consistency. Declarative memory odor cueing was associated with a decreased phase coupling consistency (Odor D vs Odor M: -0.20 ± 0.01 vs 0.03 ± 0.02, average ± SEM, p = 0.025, z = 2.243, **Figure 4F**), presumably as a result of the largest relative increases occurring in the bins right before and after the SO positive peak, widening the preferred phase angle. In line with this assumption, odor cueing did not significantly drive changes in the preferred phase angle of coupled events (13.51 ± 6.25° vs 3.08 ± 8.78°, p = 0.281, F = 1.191, **Figure 4G**).

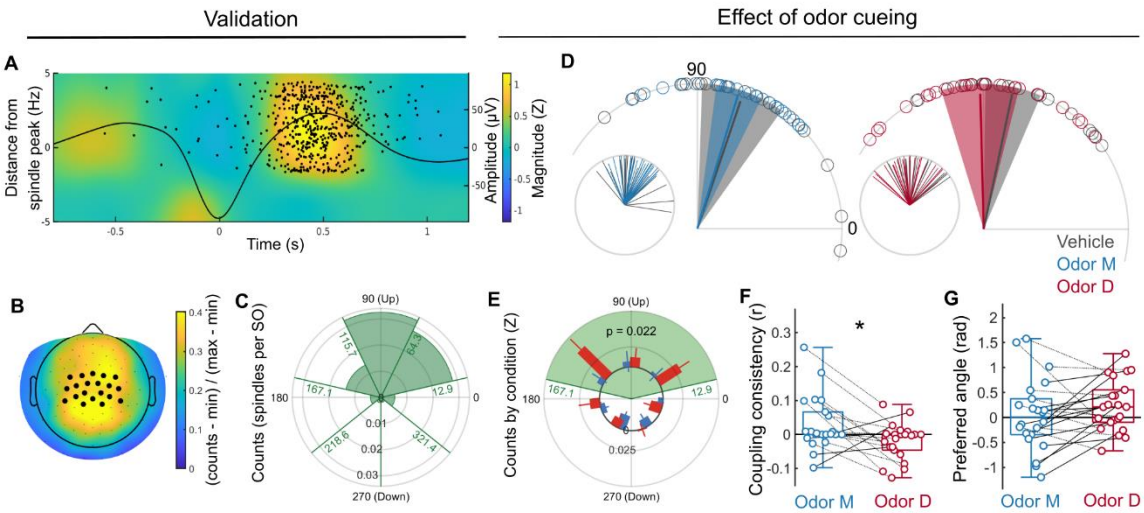

Figure 4: Odor cueing leads to accumulation of sleep spindles around slow oscillatory up states. A*, Time-frequency representation of spindle activity around slow oscillations. Shown is the power over central areas (see black circles in panel **B**) at frequencies ± 5 Hz centered around the average spindle peak frequency across subjects (13.80 Hz). Black waveform shows grand average slow oscillation, black dots indicate spindle midpoints (arbitrary vertical distribution). **B****, Most coupled events were detected in and around central electrodes (colors show spindle counts per slow oscillation, black circles show analyzed electrodes for all other panels of this figure). **C****, Visualization of spindle counts per detected SO event (dark green bars, conditions and both nights combined), separated by SO phase (first 7.5 s of odor stimulation; bin size: 51.4°; bin edges marked in green). **D****, Preferred phase angle for each participant (circles on polar axis and vector direction in inlays) as well as coupling strengths (vector lengths in inlays) for each condition. Magnified figures indicate the preferred phase angle and 95 % confidence intervals across subjects. **E****, Changes in bin counts (Z-scores* ± SEM*) by odor cueing in phase bins. Statistical significance is shown for the analysis of averages across bins between 12.9° and 167.1° (green background) which is the phase range considered in **F** and **G**. **F****, Subjects' phase coupling consistency (vector length, r). **G****, Odor-induced changes in the preferred SO phase angle of coupled spindles. *, p = 0.025. Lines connect data points from the same participant.*

Declarative memory cueing Increased spectral power for SW, and theta band around odor onset

In addition to isolated event analyses, we performed a power analysis to detect potentially more continuous brain responses in the most prominent frequency bands during NREM sleep. Based on the event-based results presented above, we restricted our power analysis to central electrodes (same as in **Figure 4B**). Our results showed no robust changes across most of the stimulation period with the exception of the time right around odor onset. There, an unexpected increase in power emerged for the SW (Odor D vs Odor M, -1 s to 1.1 s, 0.09 ± 0.15 vs -0.03 ± 0.11, average ± SEM, cluster-level p = 0.036) and theta bands (-0.5 to 0.4 s, 0.07 ± 0.14 vs -0.05 ± 0.09, p = 0.029) (**Figure 5**) (all cluster-level p > 0.05). Visual inspection of single-trial data showed that these transient power increases likely correspond to a slightly higher likelihood of slow wave occurrences around odor onset. There was no precise time-locked event related potential (ERP) visible in the across-trial average. Such time-locked responses would be expected, e.g., if the higher number of slow waves were the result of inadvertent audible noise at odor onset.

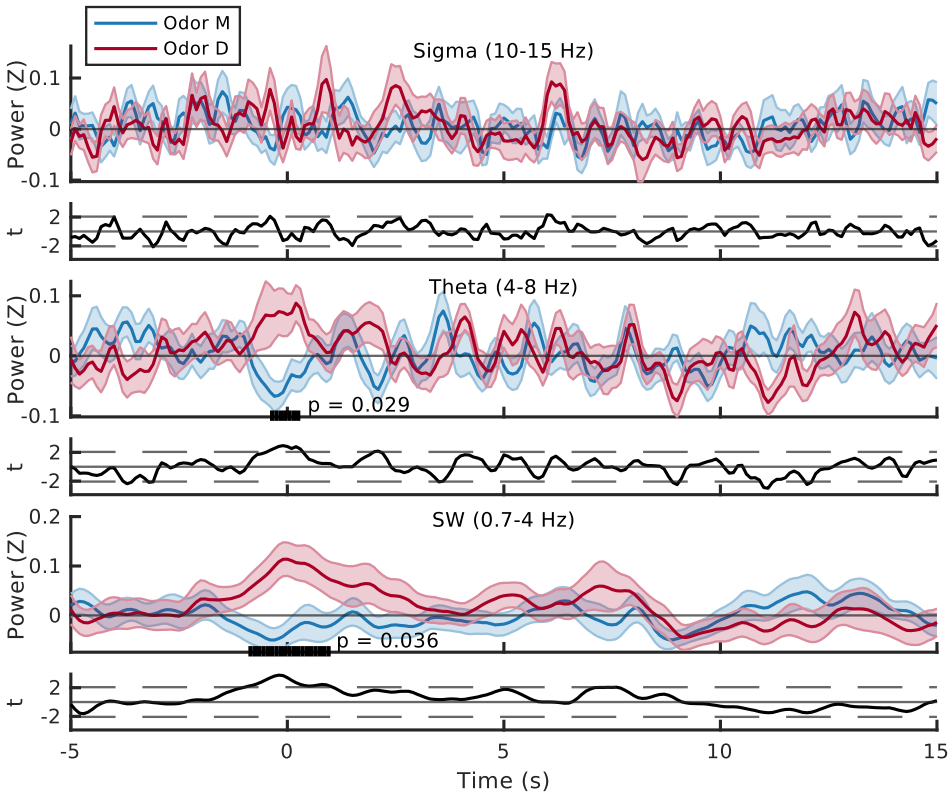

Figure 5: Low-frequency power increases around the time of odor onset. *Time-series of normalized power in frequency bands of interest. For each frequency band, the upper panel*

contains the time series for Odor M (blue) and Odor D (red), and the lower panel provides the t-value for each time point when statistically comparing the two conditions. Dashed horizontal lines show the critical values at -2.0739 and 2.0739. The black horizontal bars along the x-axis represent significance after a cluster permutation procedure in the time domain (sample-level p = 0.05).

No significant differences in memory performance, sleep architecture, or sleep quality

While electrophysiological features revealed changes when comparing the two stimulation conditions, there were no significant differences in memory performance (Night D vs Night M: 75.61 ± 5.38 vs 75.13 ± 4.22, average ± SEM (performance), p = 0.956, Wilcoxon's z = 0.055, **Supplementary Figure 1**). Also the distribution of sleep stages was comparable between conditions (Table 1). On average, subjects showed slightly more N1 in the Odor D night (Night D vs Night M: 6.61% vs 3.92%, uncorrected p = 0.008; see Table 1), with this small difference being very unlikely to influence overall results. Subjects tended to be in deeper sleep stages (S4, Night D vs Night M: 17.42 vs 22.59, average (%), uncorrected p = 0.052) and to spend less time awake after sleep onset (WASO, Night D vs Night M: 3.74 vs 2.35, average (%), uncorrected p = 0.059). Please note that all these tests are reported uncorrected for multiple comparisons to maximize statistical sensitivity.

	M Night	D Night	p value (uncorrected)
Sleep onset (min)	11.89 ± 1.24	12.17 ± 1.22	0.825
TST (min)	57.41 ± 3.37	57.46 ± 3.29	0.992
S1 (%)	3.92 ± 0.49	6.61 ± 0.87	0.008 *
S2 (%)	30.36 ± 3.55	29.23 ± 3.13	0.704
S3 (%)	23.65 ± 2.49	26.53 ± 2.60	0.110
S4 (%)	22.59 ± 3.50	17.42 ± 3.23	0.052
SWS (%)	46.24 ± 3.07	43.95 ± 3.11	0.422
REM (%)	0.41 ± 0.41	0 ± 0	0.328
WASO (%)	2.35 ± 0.46	3.74 ± 0.72	0.059
Arousals (#)	6.61 ± 1.57	5.70 ± 1.18	0.526
SE	80.94 ± 1.93	79.80 ± 1.82	0.491

***Table 1.* Sleep architecture across experimental conditions.** *Conditions did not differ in terms of important characteristics of sleep, incl. the proportion of sleep spent in each sleep stage. Arousals, Number of awakenings after sleep onset; REM, Rapid Eye Movement sleep; S1-4, Non-Rapid Eye Movement sleep stages 1 to 4; SE, Sleep efficiency (percentage of sleep after lights out); Sleep onset, Latency of first sleep score after lights out; SWS, Slow-wave sleep; TST,*

Total sleep time; WASO, Wake after sleep onset. Values are expressed as averages ± SEM. Only one significant difference emerged (S1, p = 0.008 uncorrected; parametric t-test), which did not survive multiple comparison correction.

Discussion

In the present study, we investigated the neural signatures associated with odor cueing of declarative memories during NREM sleep. To this goal, we compared electrophysiological features to cueing with an odor that was associated with training on a declarative memory task against cueing with an odor that was associated with sensory-motor learning. Specific to the odor associated with declarative memories, cueing increased the rate of the sleep spindles in centro-parietal areas, as well as spindle duration and amplitude in the frontal areas. Furthermore, the coupling between SOs and spindles was enhanced, such that spindles accumulated at higher rates around the SO up states. Cueing declarative memories also led to power increases in the slow wave and theta frequency bands. Surprisingly, this increase happened near the odor onset. In summary, using a well-controlled olfactory cueing design, we show that declarative memory-associated odor cues induce intricate changes in activity across widespread brain areas. Characterizing these changes is an important step towards a better understanding of the neural underpinnings of both cued and spontaneous memory consolidation.

Since its initial demonstration[4], the beneficial effect of memory cueing using odors has been shown for creativity tasks[26], fear extinction[16], declarative memory in a real-life setting[27,28]. The beneficial effect of cueing on memory has been shown to be odor-specific[15,29], can be expressed unilaterally in the brain[14], and is protected against interference when applied during sleep[5,29–31]. While in the current study, the effects of declarative memory odor cueing on brain activity were not expressed in significantly improved declarative memory performance (**Supplementary Figure 1**), this does not preclude the presence of robust electrophysiological signatures of the induced memory processes, as demonstrated in prior studies[13,12]. However, electrophysiological evidence for the effects of odor cueing is sparse.

When it comes to discrete events, two studies have shown an increase of spindle density in parietal[12] and occipital areas[13]. The present study reveals changes in spindle rate over more widespread areas, as well as amplitude changes over frontal instead of only occipital areas.

Such differences are not surprising, as sleep spindles are rather local events and their topology may change according to the learned content, details of its presentation (e.g., location in the visual field), and details of the cueing. Concerning SOs, our observations show a trend for an increase in trough amplitude in response to declarative memory odor cueing. We did not see effects on negative-to-positive slopes of SOs as shown by Rihm et al.[15] Turning to temporal coupling of SOs and spindles, cueing-evoked changes in this coupling have been shown in several auditory stimulation studies, where the cue itself is likely to elicit an SO and a nested spindle state[32,33]. Only one study so far has revealed changes in phase-amplitude coupling in response to odor cueing[14]. In this study, memory cueing resulted in spindles occurring later along the SO, tightly locked to their up states, particularly over frontal areas. While our study did not reproduce such a shift, we observed reduced coupling consistency, likely being attributable to *de novo* generated spindles around SO up states (see results section about accumulation of spindles around SO up states).

When looking at frequency bands rather than discrete events, we did not detect differences between the stimulation conditions in the spindle band, while such changes had been observed in other studies (Rihm et al. 2014, 2016; Bar et al. 2020). Different approaches to data normalization (see discussion below), as well as the choice of baseline periods could account for these differences in results. Responses in low frequencies have been shown by other studies[15,30,14]. However, it is surprising that in our study, declarative memory odor cueing evoked a response right at odor onset since, despite a constant airflow towards the participant to which either odor or vehicle is added, we would not expect the odor release to be noticeable until the next inhalation cycle. We can exclude that our finding is a general evoked response to odor because all comparisons were performed against a control odor. Extra care was also taken to ensure the same air flow across all conditions (e.g., by equalizing pipe length and number of pipe branches for all odor sources). We can further exclude an auditory-evoked potential, e.g., by different valves in the olfactometer making more or less noticeable sounds, as these were counterbalanced across subjects and nights. Auditory-evoked slow waves would also be expected to be time-locked more precisely than observed in the data. A speculative explanation for the phenomenon would be that the power increase represents an anticipatory response to the odor, which might be stronger for memory-associated cues.

Normalization and statistical contrast. In the present study, experimental paradigm and data analysis strategies were designed to maximize control for potential confounding factors. Previous studies have often used the breaks in between stimulations (sometimes called "odor-off" periods) to normalize responses to stimulation, and another (sham or vehicle-only) night as the control condition. In our strategy, vehicle time periods used for normalization are separated from the odor periods by a post-stimulation break of the same length. We believe this approach provides a cleaner comparison, since brain activity elicited by the odor could still persist after odor offset. Normalized data were contrasted against a control, which was performed in the other night, in which stimulation was performed with another familiar odor instead of no odor or mere vehicle. These control data were itself normalized by a vehicle condition during the same night. This strategy controls for differences between individuals, nights, odor familiarity, memory-unspecific effects of odors, and, because vehicle periods were interleaved with odor periods, also for time-of-night effects.

Limitations and future research. An important limitation of the current study is the intrinsic temporal vagueness of the olfactory cueing modality. The odor takes time to travel through the pipes and its perception is subject to the respiratory rhythm[34]. Improved ways to release odors with high temporal accuracy together with respiratory monitoring could alleviate this problem in future studies, resulting in greater temporal consistency across stimulation trials. Another general limitation of the olfactory cueing modality is that odors may not allow the targeting of specific memory items (e.g., single card pairs). This argument is based on the assumption that odors are rather general cues that indiscriminately reactivate the entire learning context[9]. This idea might also explain the lack of behavioral performance differences between the experimental conditions. Both odors may have indiscriminately benefitted memories of the few hours before sleep. Even if not paired directly, also Odor M may thus have inadvertently improved performance on the declarative memory task. Another explanation may simply be low statistical power common to most neuroscientific studies. Also, testing for performance differences soon after the cueing intervention might have obscured effects on memory. In support of this argument, two recent studies have shown an expression of behavioral effects of auditory memory cueing only after several hours[32] or even days[35]. In one of these studies, the category of the cued memory items could be decoded during cueing-evoked neural responses, while improvements in memory only emerged after

another full night of sleep[32]. Nevertheless, the lack of a behavioral expression of potential effects of memory cueing theoretically allows for the possibility that the observed electrophysiological characteristics are not directly related to memory reactivation. However, as our results are broadly in line with prior cueing-induced changes in studies that showed a behavioral effect[14,15], we assign a rather low likelihood to this scenario.

In summary, we extend the sparse prior literature on the neural effects of odor cueing by analyzing intricate characteristics of sleep rhythms and changes in SO-spindle phase relationships in response to stimulation. We demonstrate that cueing with a declarative memory-associated odor increases the rate and duration of sleep spindles over widespread brain areas and specifically around SO up states. We hope that our results pave the way for the use of odor cueing in electrophysiological investigations of memory consolidation, in addition to the more frequently used auditory approach.

Acknowledgments:

This research was financially supported by the ANID FONDECYT Regular grant 1171320, year 2017. Additionally, A.S-C. was financially supported by the scholarship BECAS DE DOCTORADO VRI – ESCUELA DE GRADUADOS, Pontificia Universidad Católica de Chile. D.M.B. was funded by ANID FONDECYT Postdoctorado grant 3200051, year 2020 and G.A.W. was supported in part by the Centro Basal FB0008. J.G.K., S.H., and J.B. were supported by grants from the Deutsche Forschungsgemeinschaft (German Research Council, Tr-SFB 654 “Sleep and Plasticity”).

Declaration of interest:

J.G.K. is an employee of the neurotechnology company Bitbrain. D.M.B. is the CTO of the neurotechnology company Helment. Neither company influenced this study or the manuscript.

References

1. Klinzing, J. G., Niethard, N. & Born, J. Mechanisms of systems memory consolidation during sleep. *Nat Neurosci* **22**, 1598–1610 (2019).

2. Diekelmann, S. & Born, J. The memory function of sleep. *Nat Rev Neurosci* **11**, 114–126 (2010).

3. Dudai, Y. The restless engram: consolidations never end. *Annu Rev Neurosci* **35**, 227–247 (2012).

4. Rasch, B., Büchel, C., Gais, S. & Born, J. Odor cues during slow-wave sleep prompt declarative memory consolidation. *Science* **315**, 1426–1429 (2007).

5. Diekelmann, S., Büchel, C., Born, J. & Rasch, B. Labile or stable: opposing consequences for memory when reactivated during waking and sleep. *Nat Neurosci* **14**, 381–386 (2011).

6. Rudoy, J. D., Voss, J. L., Westerberg, C. E. & Paller, K. A. Strengthening individual memories by reactivating them during sleep. *Science* **326**, 1079 (2009).

7. Antony, J. W., Gobel, E. W., O'Hare, J. K., Reber, P. J. & Paller, K. A. Cued memory reactivation during sleep influences skill learning. *Nat Neurosci* **15**, 1114–1116 (2012).

8. Schönauer, M., Geisler, T. & Gais, S. Strengthening procedural memories by reactivation in sleep. *J Cogn Neurosci* **26**, 143–153 (2014).

9. Klinzing, J. G. & Diekelmann, S. Cued Memory Reactivation: A Tool to Manipulate Memory Consolidation During Sleep. in *Handbook of Behavioral Neuroscience* vol. 30 471–488 (Elsevier, 2019).

10. Zelano, C. & Sobel, N. Humans as an animal model for systems-level organization of olfaction. *Neuron* **48**, 431–454 (2005).

11. Carskadon, M. A. & Herz, R. S. Minimal olfactory perception during sleep: why odor alarms will not work for humans. *Sleep* **27**, 402–405 (2004).

12. Rihm, J. S., Sollberger, S. B., Soravia, L. M. & Rasch, B. Re-presentation of Olfactory Exposure Therapy Success Cues during Non-Rapid Eye Movement Sleep did not Increase Therapy Outcome but Increased Sleep Spindles. *Front Hum Neurosci* **10**, 340 (2016).

13. Cox, R., Hofman, W. F., de Boer, M. & Talamini, L. M. Local sleep spindle modulations in relation to specific memory cues. *Neuroimage* **99**, 103–110 (2014).

14. Bar, E. *et al.* Local Targeted Memory Reactivation in Human Sleep. *Current Biology* **30**, 1435-1446.e5 (2020).

15. Rihm, J. S., Diekelmann, S., Born, J. & Rasch, B. Reactivating memories during sleep by odors: odor specificity and associated changes in sleep oscillations. *J Cogn Neurosci* **26**, 1806–1818 (2014).

16. Hauner, K. K., Howard, J. D., Zelano, C. & Gottfried, J. A. Stimulus-specific enhancement of fear extinction during slow-wave sleep. *Nat Neurosci* **16**, 1553–1555 (2013).

17. Diekelmann, S., Biggel, S., Rasch, B. & Born, J. Offline consolidation of memory varies with time in slow wave sleep and can be accelerated by cuing memory reactivations. *Neurobiol Learn Mem* **98**, 103–111 (2012).

18. Klinzing, J. G. *et al.* Spindle activity phase-locked to sleep slow oscillations. *NeuroImage* **134**, 607–616 (2016).

19. Rechtschaffen, A. & Kales, A. *A Manual of Standardized Terminology, Techniques and Scoring System for Sleep Stages of Human Subjects*. (Public Health Service, US Government Printing Office, Washington DC., 1968).

20. Oostenveld, R., Fries, P., Maris, E. & Schoffelen, J.-M. FieldTrip: Open source software for advanced analysis of MEG, EEG, and invasive electrophysiological data. *Comput Intell Neurosci* **2011**, 156869 (2011).

21. Wen, H. & Liu, Z. Separating Fractal and Oscillatory Components in the Power Spectrum of Neurophysiological Signal. *Brain Topogr* **29**, 13–26 (2016).

22. Ciuparu, A. & Mureşan, R. C. Sources of bias in single-trial normalization procedures. *Eur J Neurosci* **43**, 861–869 (2016).

23. Maris, E. & Oostenveld, R. Nonparametric statistical testing of EEG- and MEG-data. *J Neurosci Methods* **164**, 177–190 (2007).

24. Maris, E., Schoffelen, J.-M. & Fries, P. Nonparametric statistical testing of coherence differences. *J Neurosci Methods* **163**, 161–175 (2007).

25. Berens, P. **CircStat** : A *MATLAB* Toolbox for Circular Statistics. *J. Stat. Soft.* **31**, (2009).

26. Ritter, S. M., Strick, M., Bos, M. W., van Baaren, R. B. & Dijksterhuis, A. Good morning creativity: task reactivation during sleep enhances beneficial effect of sleep on creative performance. *J Sleep Res* **21**, 643–647 (2012).

27. Neumann, F., Oberhauser, V. & Kornmeier, J. How odor cues help to optimize learning during sleep in a real life-setting. *Sci Rep* **10**, 1227 (2020).

28. Vidal, V. *et al.* Odor cueing during sleep improves consolidation of a history lesson in a school setting. *Sci Rep* **12**, 10350 (2022).

29. Shanahan, L. K., Gjorgieva, E., Paller, K. A., Kahnt, T. & Gottfried, J. A. Odor-evoked category reactivation in human ventromedial prefrontal cortex during sleep promotes memory consolidation. *eLife* **7**, e39681 (2018).

30. Klinzing, J. G. *et al.* Odor cueing during slow-wave sleep benefits memory independently of low cholinergic tone. *Psychopharmacology (Berl)* **235**, 291–299 (2018).

31. Seibold, M., Rasch, B., Born, J. & Diekelmann, S. Reactivation of interference during sleep does not impair ongoing memory consolidation. *Memory* **26**, 377–384 (2018).

32. Cairney, S. A., Guttesen, A. Á. V., El Marj, N. & Staresina, B. P. Memory Consolidation Is Linked to Spindle-Mediated Information Processing during Sleep. *Curr Biol* **28**, 948-954.e4 (2018).

33. Schreiner, T., Petzka, M., Staudigl, T. & Staresina, B. P. Endogenous memory reactivation during sleep in humans is clocked by slow oscillation-spindle complexes. *Nat Commun* **12**, 3112 (2021).

34. Kepecs, A., Uchida, N. & Mainen, Z. F. The Sniff as a Unit of Olfactory Processing. *Chemical Senses* **31**, 167–179 (2006).

35. Rakowska, M., Abdellahi, M. E. A., Bagrowska, P., Navarrete, M. & Lewis, P. A. Long term effects of cueing procedural memory reactivation during NREM sleep. *Neuroimage* **244**, 118573 (2021).